nature ecology & evolution

SUPPLEMENTARY INFORMATION

VOLUME: 1 | ARTICLE NUMBER: 0177

In the format provided by the authors and unedited.

Competition-induced starvation drives large-scale population cycles in Antarctic krill

Alexey B. Ryabov[1]*, André M. de Roos[2], Bettina Meyer[1,3,4], So Kawaguchi[5,6] and Bernd Blasius[1,4]

Affiliations:

[1]Institute for Chemistry and Biology of the Marine Environment, University of Oldenburg, Oldenburg, Germany

[2]Institute for Biodiversity and Ecosystem Dynamics, University of Amsterdam, The Netherlands

[3]Alfred Wegener Institute for Polar and Marine Research, Scientific Division Polar Biological Oceanography, Bremerhaven, Germany

[4]Helmholtz Institute for Functional Marine Biodiversity at the University of Oldenburg, Germany, www.hifmb.de

[5]Australian Antarctic Division, Kingston, Tasmania, Australia

[6]Antarctic Climate and Ecosystems Cooperative Research Centre, Hobart, Australia.

*Correspondence to: alexey.ryabov@uni-oldenburg.de.

Content:

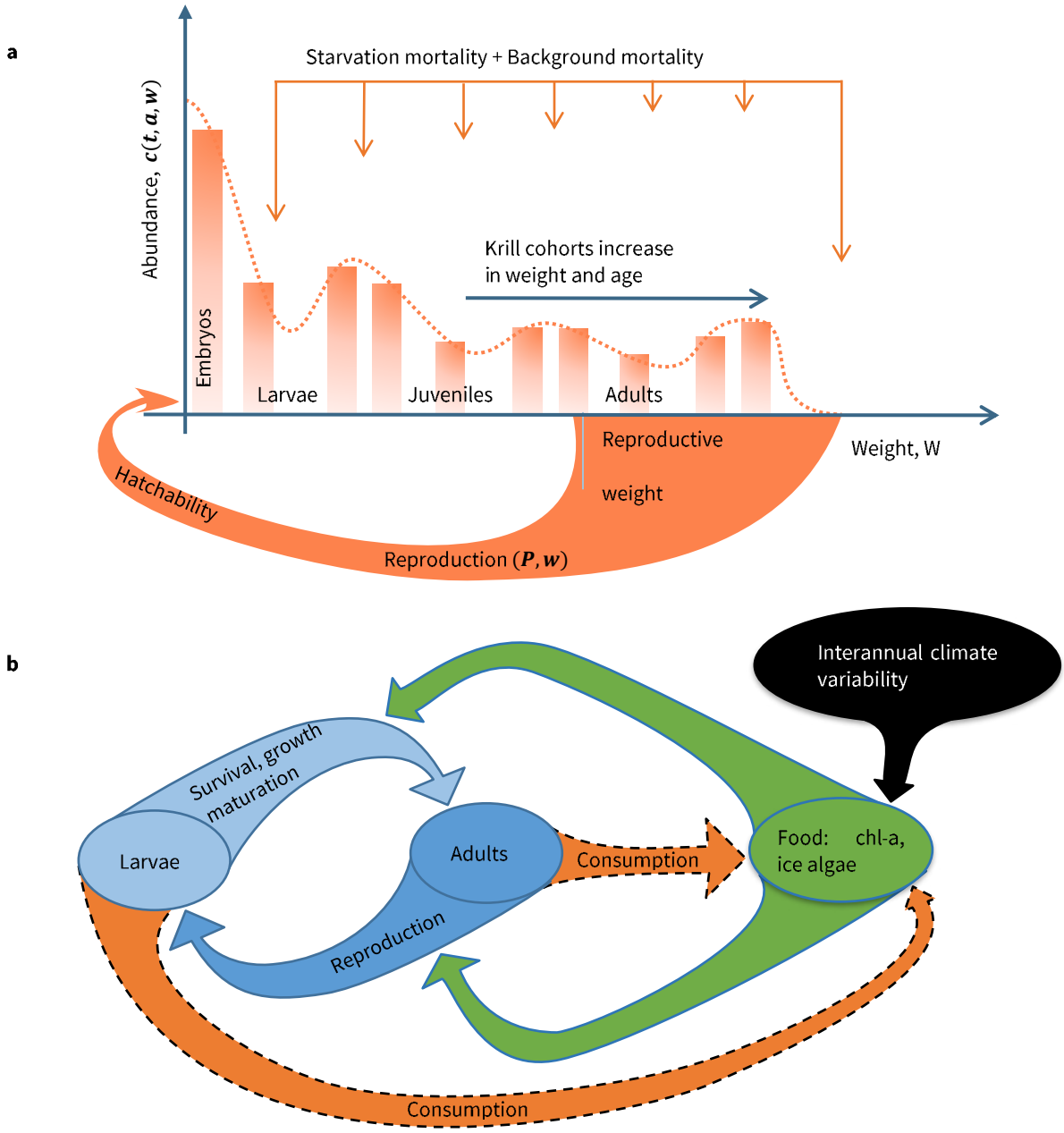

Supplementary Figure 1. The ontogenetic modeling of krill population dynamics and the interactions between krill cohorts and the environment. a, Krill cohorts (orange bars) increase their weight and move from left to right along the weight axis. The dotted orange line shows the krill weight distribution $c(t, a, w)$. **b**, The interaction between krill cohorts and the environment. The traditional concept suggests that fluctuations in krill abundance follow the changes in food level caused by periodical environmental changes (black arrow). Our study complements this approach and shows that the feedback of krill biomass on the food level (highlighted by black dashed outlines) plays a crucial role in the appearance of krill population cycles.

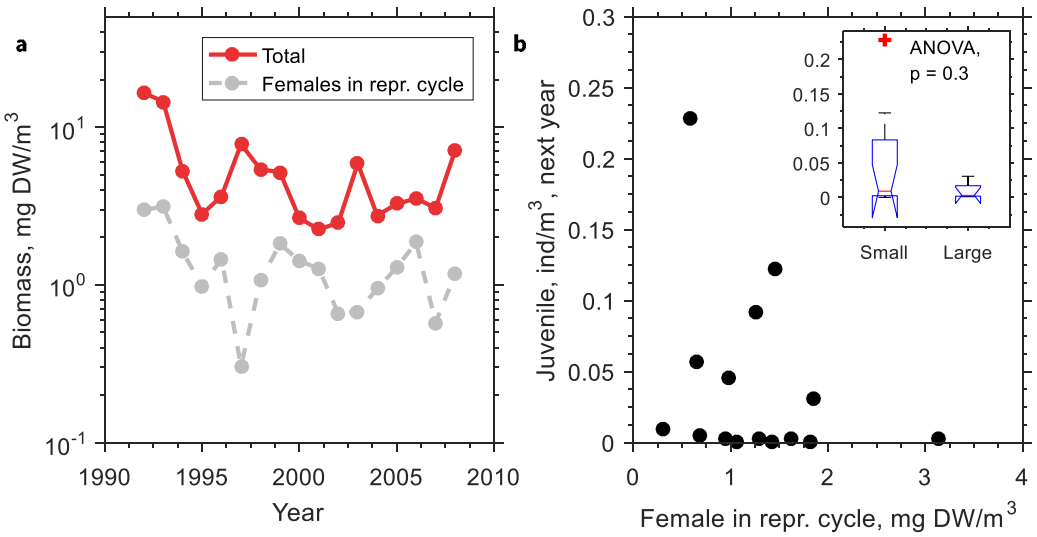

Supplementary Figure 2. Krill reproductive capacity. a, Temporal changes in the biomass of females with red thelycum (i.e., in reproductive cycle, grey dashed line) compared to total krill biomass (red). Total biomass of females in reproductive cycles depends on krill abundance, length distribution and available food. The maxima of reproductive female biomass do not coincide with the maxima in total biomass as the reproductive female biomass is large when an abundant strong krill cohort reaches larger sizes and when summer conditions are favorable for reproduction. **b,** The abundance of juveniles decreases with the biomass of female in reproductive cycle in the preceding year. The inset shows a box plot of the same data divided into two groups (Small, Large) with the female biomass either smaller or larger than 1.5 mg DW/m^3 (insignificant, $p = 0.3$).

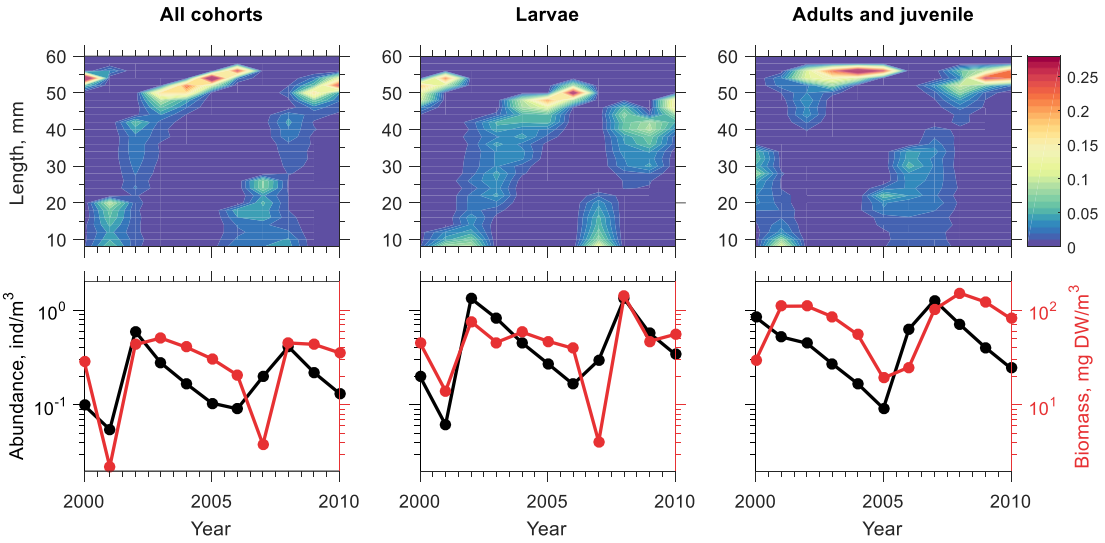

Supplementary Figure 3. Robustness of the krill cycles to different grazing modes. Simulated population cycles when phytoplankton is consumed by all cohorts (left), only by larvae (adults and juveniles are still limited by the same phytoplankton, middle), or only by adults and juveniles (larvae are limited by the same phytoplankton, right). The figures show oscillations in the length distribution in color coding **(top)** and abundances (black lines) and biomass (red lines) **(bottom)**.

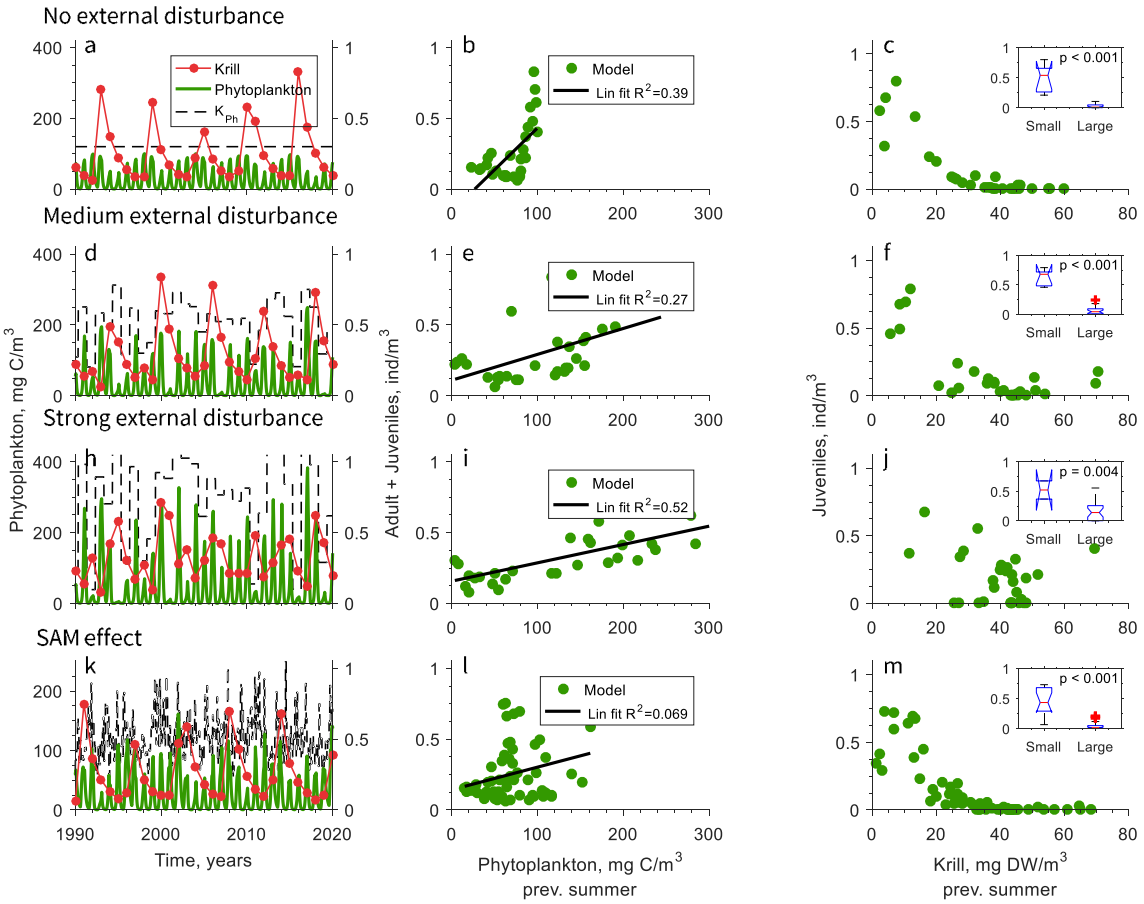

Supplementary Figure 4. Sensitivity of the krill cycle to inter-annual environmental variability. Environmental disturbances are simulated as random inter-annual changes in phytoplankton carrying capacity K_{Ph} in a gradient from unperturbed to strongly perturbed (three upper rows) and assuming that phytoplankton carrying capacity, K_{Ph}, is driven by Southern Annular Oscillations index[9], namely, $K_{Ph} = K_{Ph,0}\exp(-0.3\ \mathrm{SAM})$ (bottom). (Left panel) Time course of simulated phytoplankton carrying capacity (black dashed line), phytoplankton concentration (green) and total krill abundance (red line). (Middle panel) Relation between summer phytoplankton concentration and krill abundance in the following year (green dots) and linear regression (black line). (Right panel) Relation between krill biomass and juvenile abundance in the following year (green dots, compare to Fig. 1h). The insets show a box plot of the same data divided into two groups (Small, Large) with the total krill biomass either smaller or larger than 20 mg DW/m^3. See Methods (Environmental interannual disturbances) for model parameters.

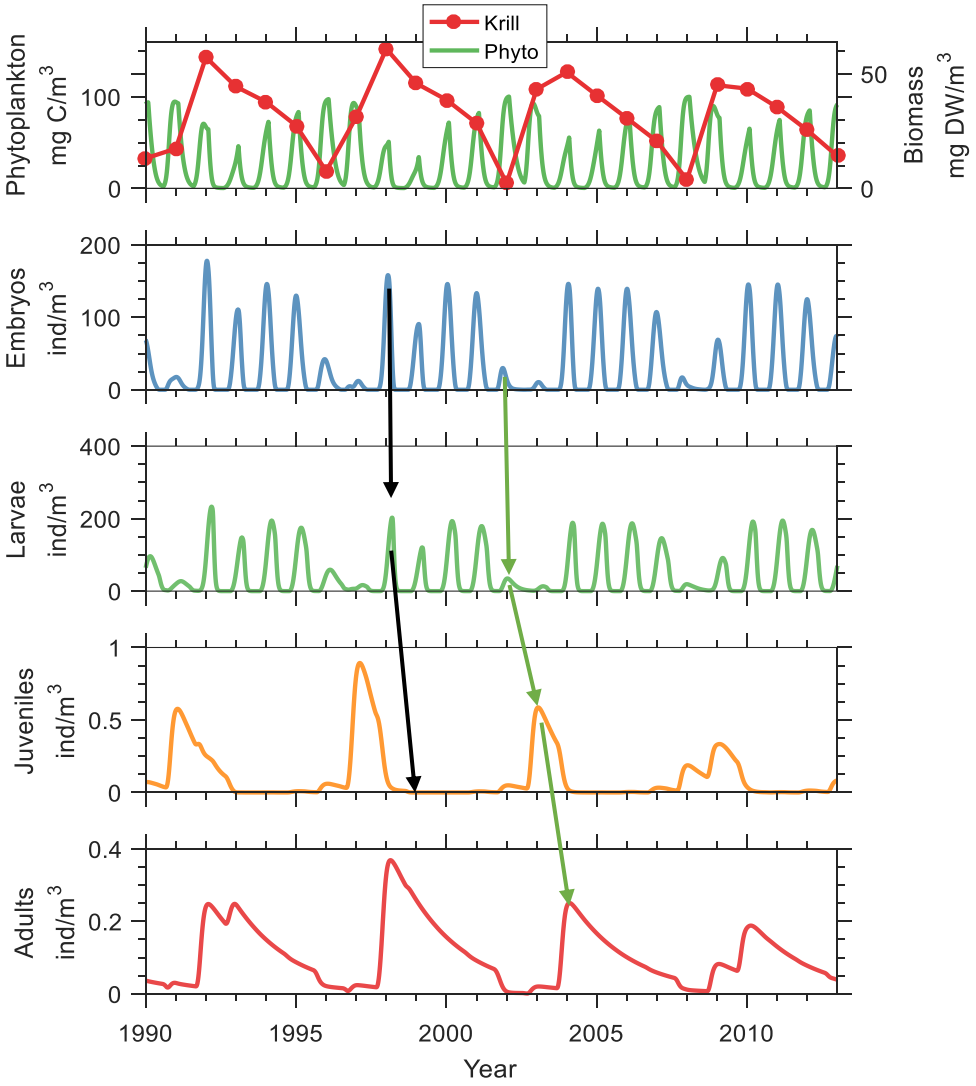

Supplementary Figure 5. The modeled dynamics of phytoplankton, krill biomass and different krill stages. a, The annual maxima of phytoplankton concentrations (green line) correlate with the annual minima of total biomass (adults + juveniles) and *vice versa*. **b**, Embryo abundances approximately follow the pattern for total krill biomass, because reproduction is not food limited. **c,** The maximal abundance of larvae is proportional to the number of embryos with a 30 days delay. However, the number of larvae can subsequently drop abruptly if autumn phytoplankton concentration is extremely low. The model predicts no positive relationship between the abundance of larvae at the end of summer and the abundance of juveniles at the beginning of the next summer. If autumn phytoplankton concentration is small even a big cohort of larvae does not result in substantial recruitment, and if the autumn conditions are good, a relatively small cohort of larvae can result in a strong cohort of juveniles, which become dominating adults in the following year **(d)** and increases total krill abundance **(e)**. The black, and green, arrows connect the different stages of a weak cohort which becomes extinct, and of a strong cohort, respectively

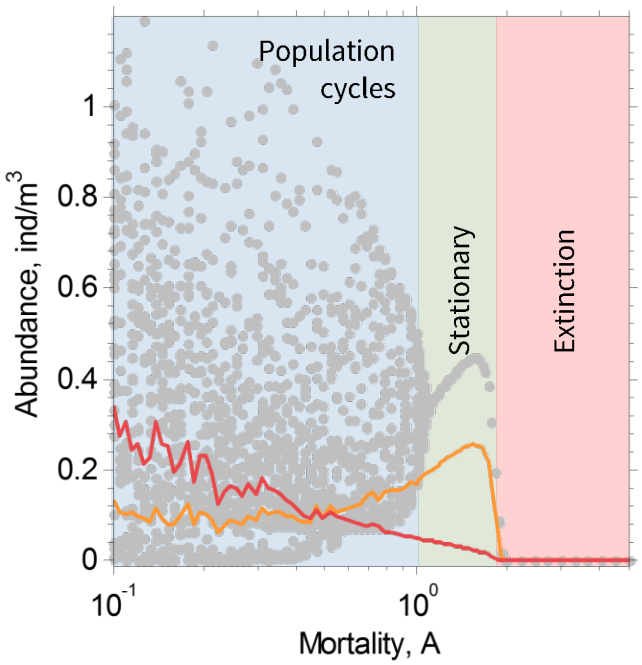

Supplementary Figure 6. The effect of krill loss rates on population dynamics. The bifurcation diagram shows the effect of krill mortality on the summer maxima of the total abundance of adult and juvenile krill (grey dots) and on the average over 50 years abundance of larvae (orange) and adults (red). The data are plotted with respect to the adult mortality, for juveniles we assumed $m_J = 2m_A$.

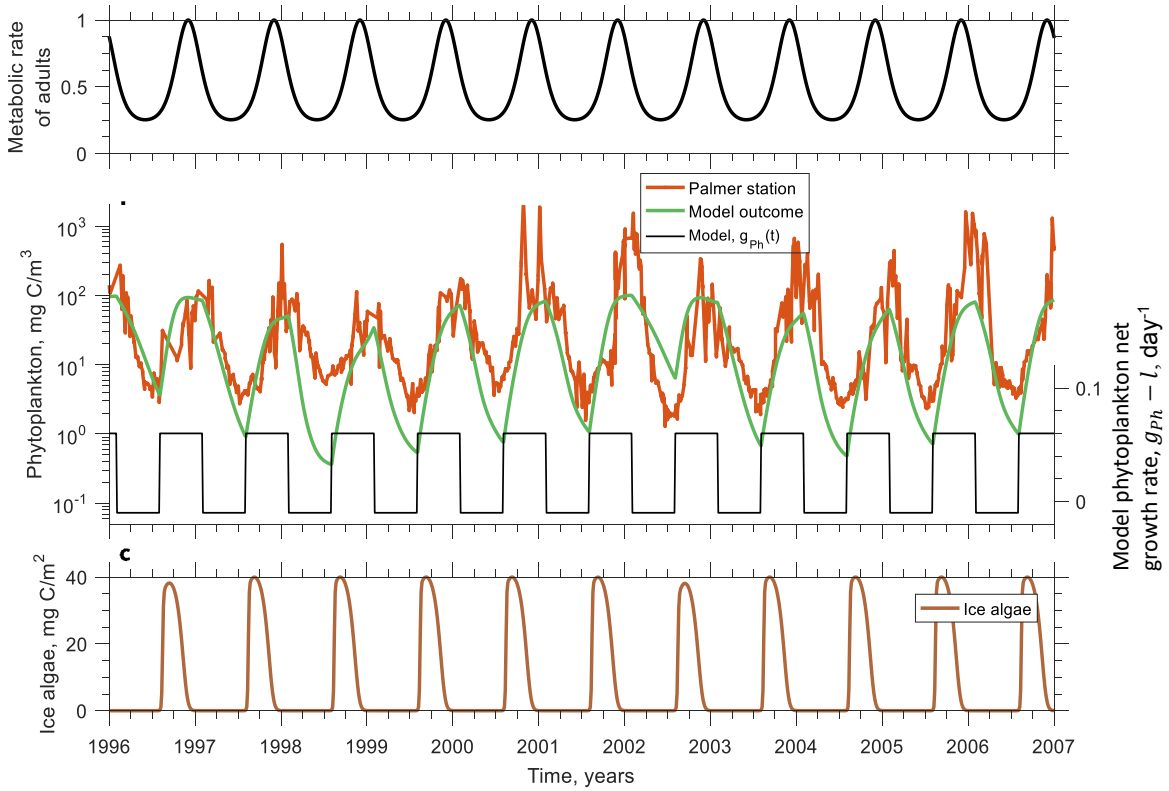

Supplementary Figure 7. The seasonal drivers of the population dynamics. The krill model integrates the combined effect of several seasonal drivers. **a,** The metabolic rate of adults. **b,** The modelled dynamics of phytoplankton concentrations (green) in the presence of krill compared to the levels of chlorophyll-a measured during 11 years at Palmer station (orange) and the net growth rate of phytoplankton (black line), as defined by equation (6). **c,** The model outcome for seasonal dependence of ice algae.

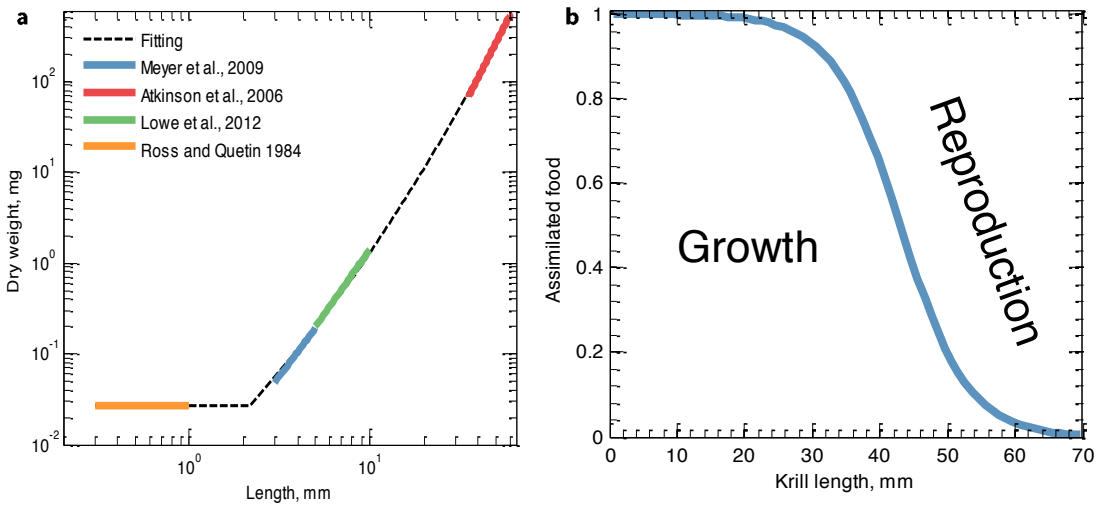

Supplementary Figure 8. Parametrization of the krill model. a, Relationship between dry weight and length of the individuals, $w = c_w \, L^{\sigma_1 + \sigma_2 \ln L}$, see parameter values in Supplementary Table 3. **b,** The splitting of the assimilated food with increasing length of the individuals into growth and reproduction processes as defined by the function $K(w) = \left(1 + e^{k\left(L(w) - L_{repr}\right)}\right)^{-1}$.

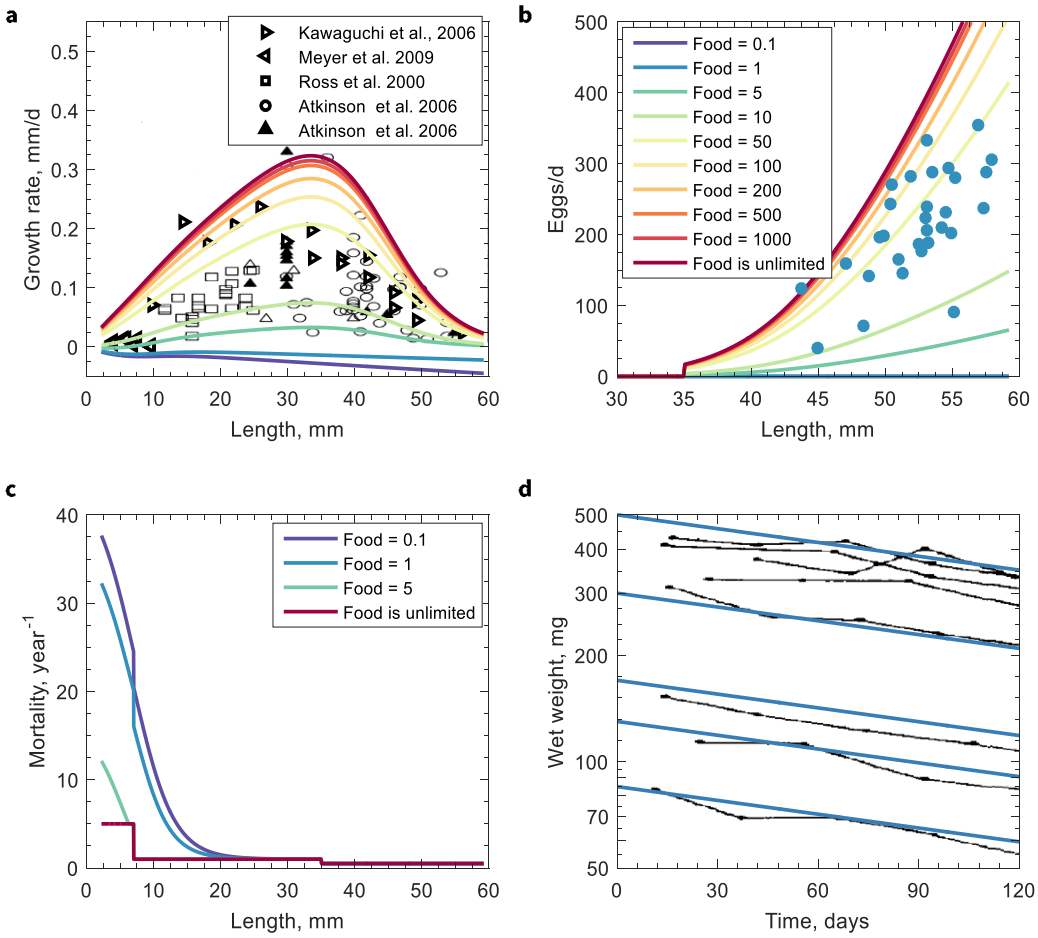

Supplementary Figure 9. Krill life traits. Comparison of the model prediction for **(a)** the daily growth rates and **(b)** daily fecundity rate for different levels of food (mg C/m^3, shown by different colors) with field data[33,34,39,45,49] (symbols). Note: Krill can shrink if the resource is less than 1 mg C/m3. **c,** Modelled krill mortality as a function of krill length for different levels of food availability. The dark red line shows the background mortality which decreases with krill size. The other lines show a sum of the background mortality and starvation mortality for different food levels. The maximal mortality is 40 year^{-1},which implies that after 14 days of starvation only approximately 20% of population survive. **d,** The dynamics of krill shrinking[17] (black lines) in comparison with the model outcome (blue lines) for starving krill.

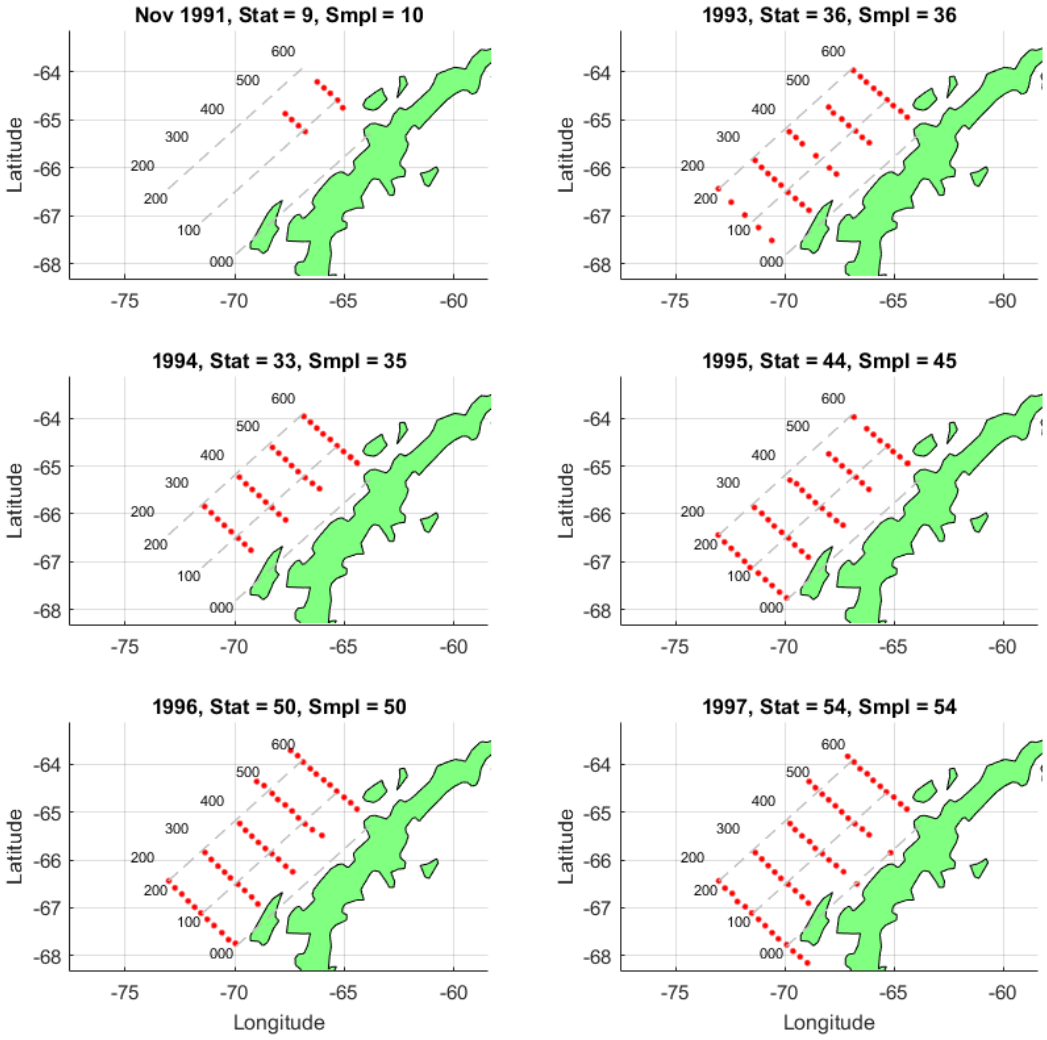

Supplementary Figure 10. A map of the LTER grid for 1991-1997. During the observational period, the data were sampled with different frequency across the LTER grid. The grid lines were spaced 100 km apart with sampling stations along every line spaced 20 km apart. The number of a grid line or a grid station shows the distance in km from line 000 or station 000, respectively. The title shows the number (n) of stations, which were sampled during the cruise, and the total number of samples, which can be larger than the number of stations when more than one sample was taken at the same location.

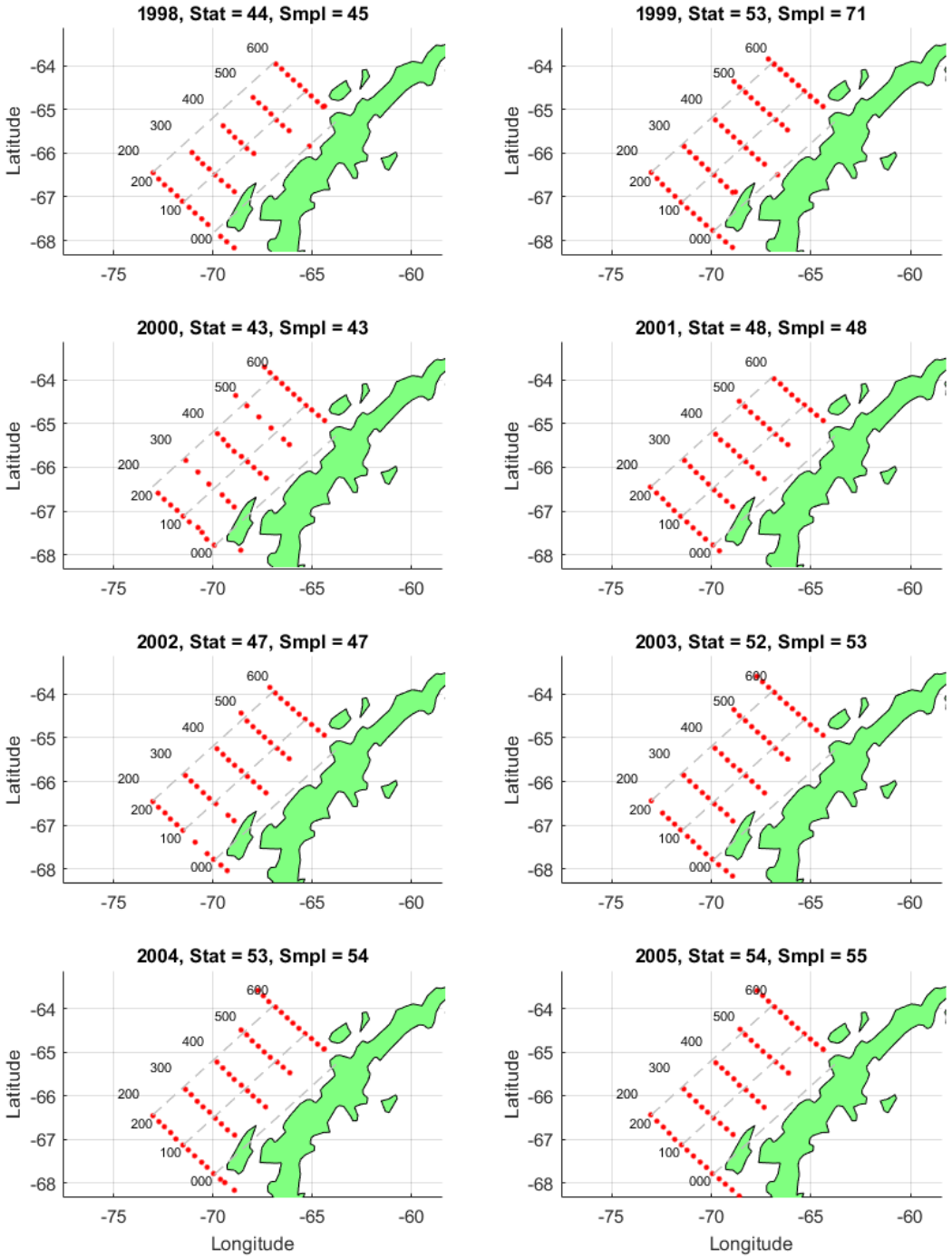

Supplementary Figures 11. The same as Fig. S10, years 1998-2005

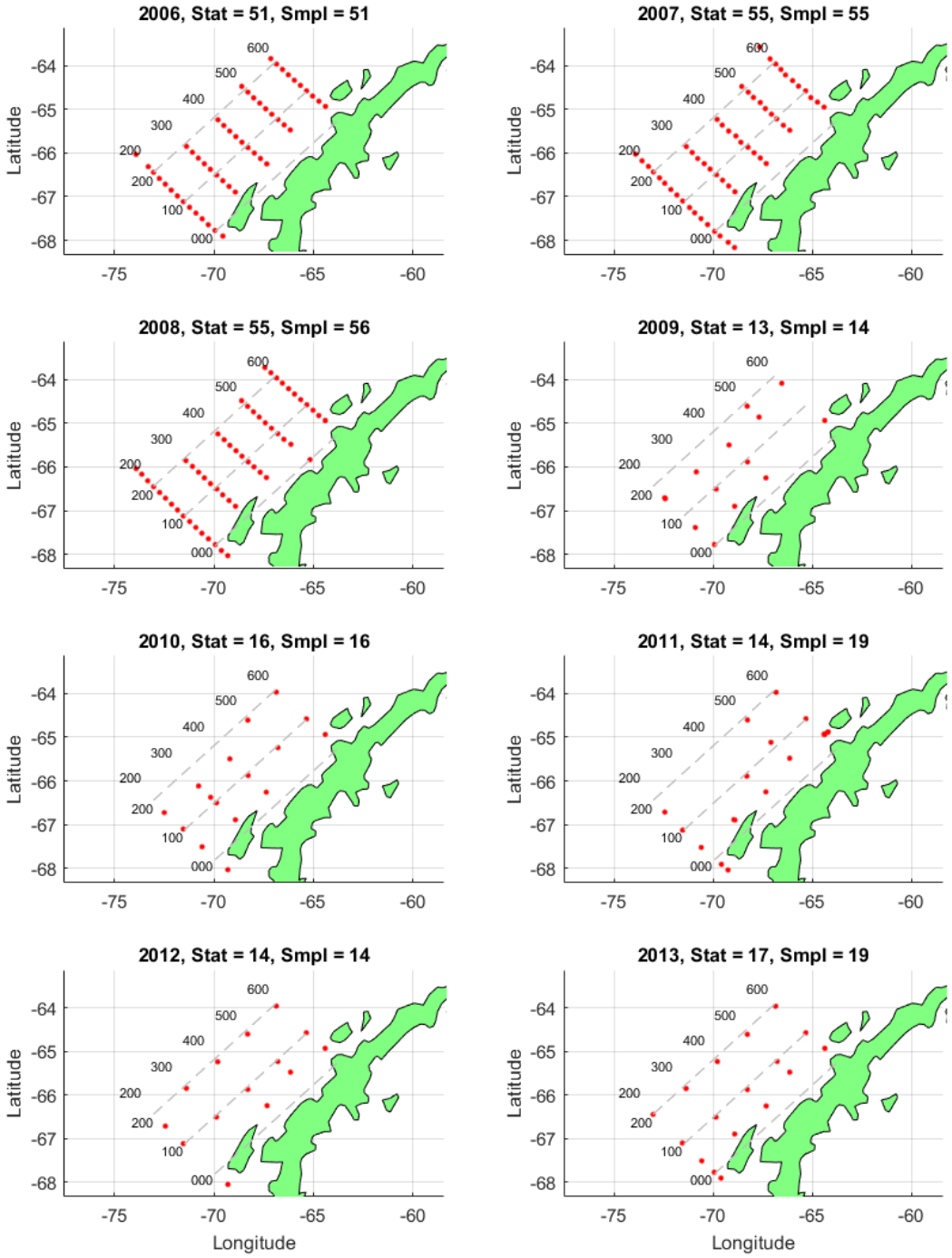

Supplementary Figures 12 The same as Fig. S10, years 2006-2013

Supplementary Table 1. Krill growth and reproduction

Parameter	Value	Units	Meaning	Source
larvae age	30	days	minimal age of larvae	
Juvenile age	1	years	The minimal age of juveniles	
Reproductive age	2	years	Minimal age for reproduction	
life span	5.9	years	krill life span	
L_l	7	mm	minimal larvae size	
k_l	1/3	mm-1		
$L_{repr,min}$	35	mm	the minimal length for reproduction	45
L_{repr}	43	mm	the length at which 50% of female reproduce	36
k_{repr}	1/5	mm-1		
L_e	0.6	mm	Egg size	32,50
w_e	0.027	mg	Egg dry weight	
ε_{ovary}	0.82		the relative weight of eggs in ovary tissue	
T	0.003	1/day	Maintenance coefficient	
T_l	0.01	d-1	Maintenance of larvae	17
d_e	5	year-1	Mortality of embryos	
d_l	5	year-1	Mortality of larvae	
d_j	1	year-1	Mortality of juveniles	46
d_a	0.5	year-1	Mortality of adults	46
d_{sl}	40	year-1	Maximal starvation mortality	

Supplementary Table 2. Krill Ingestion rate

Parameter	Value	Units	Meaning	Source
H	25	mg C/m3	Half-saturation constant for growth rate and ingestion rage	39
I_0	10	(% body C/d-1)	Maximal ingestion rate	38
ε	1.04	mg DW /mg consumed C	Assimilation efficiency of consumed carbon into dry weight	
γ_{C2DW}	0.4	mgC/mgDW	Carbon weight – dry weight	38

Supplementary Table 3 Relationship between krill length and dry weight, Eq (1)

Parameter	Value	Units	Meaning	Source
c_w	0.0058			33–35
σ_1	1.8050			
σ_2	0.2380			
L_e	0.6	mm	Egg size	32,50
w_e	0.0277	mg	Egg dry weight	

Supplementary Table 4. Parameters of carbon production

Parameter	Value	Units	Meaning
P_{Ph}		mg C/m^3	Density of phytoplankton in the water column
P_{Ice}		mg C/m^3	The density of ice algae
$C:Chl$	50	mg C/mg Chl	Carbon to chlorophyll ratio
t_{Ph}	305 (1st of November)	day of year	The midpoint of phytoplankton growth period
T_{Ph}	180	days	The duration of summer period
$g_{Ph,max}$	0.07		Maximal phytoplankton growth rate
K_{Ph}	120	mg C/m^3	Carrying capacity of phytoplankton growth
l_{Ph}	0.01	day^{-1}	Loss rate of phytoplankton
$\delta_{Ph,in}$	0.01	mg C m^{-3}day^{-1}	Inflow rate of phytoplankton from adjacent patches
t_{Ice}	250	day of year	The middle of the winter period
T_{Ice}	140	days	The duration of summer period
$g_{Ice,max}$	1	day^{-1}	Maximal growth rate of ice algae
K_{Ice}	50	mg C/m^3	Carrying capacity for ice alga
l_{Ice}	0.2	day^{-1}	Loss rate of ice algae
$\delta_{Ice,in}$	0.01	mg C m^{-3}day^{-1}	Inflow rate of phytoplankton from adjacent patches
ρ	20		The ratio of the feeding depths for larvae feeding in the water column or at the surface ice

The parameters in table S4 were chosen to fit LTER data chlorophyll dynamics, figure S7

Supplementary Table 5. Krill abundance, biomass and recruitment (Fig. 1 c, e)

Year	Recruitment 95%CI (std)	Abundance, ind/m^3 95% CI (std)	Biomass, mg DW/m^3 95% CI (std)	Number of samples, included
1991 nov	0.93± (0.029)			10
1993	0.03±0.012 (0.028)	0.23±0.06 (0.14)	18±5.4 (13)	36
1994	0.071±0.027 (0.063)	0.046±0.009 (0.021)	4.5±1.1 (2.6)	35
1995	0.22±0.029 (0.078)	0.012±0.0018 (0.0048)	1.6±0.3 (0.8)	45
1996	0.76±0.09 (0.26)	0.059±0.0072 (0.02)	3±0.51 (1.4)	50
1997	0.5±0.093 (0.27)	0.25±0.046 (0.13)	9.2±1.7 (5)	54
1998	0.11±0.031 (0.084)	0.086±0.017 (0.047)	5.8±1.1 (3)	45
1999	0.0021±0.00054 (0.0018)	0.037±0.0034 (0.011)	5.9±0.93 (3.1)	71
2000	0.066±0.024 (0.062)	0.016±0.0019 (0.0049)	2.6±0.46 (1.2)	43
2001	0.076±0.02 (0.054)	0.011±0.0012 (0.0033)	2.3±0.4 (1.1)	48
2002	0.87±0.052 (0.14)	0.11±0.016 (0.045)	2.8±0.46 (1.3)	47
2003	0.4±0.05 (0.15)	0.14±0.022 (0.063)	8.3±1.5 (4.4)	53
2004	0.13±0.041 (0.12)	0.038±0.0057 (0.017)	3.5±0.61 (1.8)	54
2005	0.086±0.018 (0.053)	0.027±0.0033 (0.0096)	3.4±0.54 (1.6)	55
2006	0.15±0.032 (0.09)	0.019±0.0025 (0.0071)	3.7±0.69 (2)	51
2007	0.66±0.069 (0.21)	0.046±0.0068 (0.02)	3±0.54 (1.6)	55
2008	0.75±0.075 (0.22)	0.3±0.058 (0.18)	11±2 (5.9)	56
2009	0.18±0.021 (0.031)	0.046±0.019 (0.029)	3.9±1.6 (2.3)	14
2010	0.16±0.031 (0.05)	0.016±0.006 (0.0096)	2.1±0.64 (1)	16
2011	0.66±0.17 (0.29)	0.028±0.0074 (0.013)	1.8±0.55 (0.97)	19
2012	0.64±0.1 (0.15)	0.42±0.22 (0.33)	8.1±2.6 (3.9)	14
2013		0.3±0.075 (0.13)		19